Application of Artificial Neural Networks for Efficient High-Resolution 2D DOA Estimation

Marija AGATONOVIĆ [1], Zoran STANKOVIĆ [1], Nebojša DONČOV [1], Leen SIT [2], Bratislav MILOVANOVIĆ [1], Thomas ZWICK [2]

[1] Dept. of Telecommunications, University of Niš, Aleksandra Medvedeva 14, 18000 Niš, Serbia
[2] Inst. für Hochfrequenztechnik und Elektronik, Karlsruhe Inst. of Technology, Engesserstr. 5, 76131 Karlsruhe, Germany

marija.agatonovic@elfak.ni.ac.rs, zoran.stankovic@elfak.ni.ac.rs, nebojsa.doncov@elfak.ni.ac.rs, leen.sit@kit.edu, bratislav.milovanovic@elfak.ni.ac.rs, thomas.zwick@kit.edu

Abstract. *A novel method to provide high-resolution Two-Dimensional Direction of Arrival (2D DOA) estimation employing Artificial Neural Networks (ANNs) is presented in this paper. The observed space is divided into azimuth and elevation sectors. Multilayer Perceptron (MLP) neural networks are employed to detect the presence of a source in a sector while Radial Basis Function (RBF) neural networks are utilized for DOA estimation. It is shown that a number of appropriately trained neural networks can be successfully used for the high-resolution DOA estimation of narrowband sources in both azimuth and elevation. The training time of each smaller network is significantly reduced as different training sets are used for networks in detection and estimation stage. By avoiding the spectral search, the proposed method is suitable for real-time applications as it provides DOA estimates in a matter of seconds. At the same time, it demonstrates the accuracy comparable to that of the super-resolution 2D MUSIC algorithm.*

Keywords

DOA estimation, MLP, RBF, sectorisation, URA.

1. Introduction

Direction of Arrival (DOA) estimation problem has been studied for many years. In mobile communications, once the direction of a user is estimated this information can be forwarded to adaptive beamforming algorithm that optimizes the radiation pattern of an antenna array. It then allocates the main beam toward the user of interest, and nulls toward users that are causing interference. Consequently, as only selected direction is targeted, the interference to adjacent cells is decreased.

A vector of received signals at linear antenna array elements is used to form a spatial covariance matrix that is the fundamental part of many DOA algorithms. Subspace based estimation methods such as MUSIC (MUltiple SIgnal Classification) [1] and ESPRIT (Estimation of Signal Parameters via Rotational Invariance Techniques) [2] are well-known of their super-resolution capability. Performing spectral search, MUSIC is able to provide accurate DOA estimates at the expense of high computational complexity. Avoiding the orthogonally search, ESPRIT demonstrates significant advantage over MUSIC as its computational complexity grows linearly with the dimension of the antenna array while that of MUSIC grows exponentially [3]. When both azimuth and elevation angular positions of a source signal have to be resolved, then rectangular antenna arrays must be employed at the receiver. Due to increased dimensionality, a time-consuming process of spatial covariance matrix eigenvalue decomposition (EVD) hinders the real-time use of subspace based algorithms such as 2D MUSIC and 2D ESPRIT.

Application of artificial neural networks (ANNs) in the area of DOA estimation is an alternative to the previously mentioned super-resolution algorithms. Performing only basic mathematical operations and calculating elementary functions, neural models are much faster than the computationally intensive DOA algorithms [4], [5]. This ability qualifies them as very suitable for determination of angular positions of source signals [6]-[11]. Employing ANNs, DOA estimation is considered as a mapping between spatial covariance matrix and DOAs. In this paper, two approaches have been used for efficient DOA estimation. The first approach is based on single RBF (Radial Basis Function) neural networks, while the second approach combines both MLP (Multi-Layer Perceptron) and RBF neural networks, trained to detect a source and to provide its high-resolution 2D DOA estimates.

In the second so-called sectorisation approach, detection of a source signal in a sector is performed using MLP networks and after that, DOA estimation is achieved with the appropriate RBF network. To reduce a training set necessary in the learning process of both network types MLP networks are trained with less data as they only perform classification of input vectors. More refined data are used to train RBF networks that provide DOA estimation. Given that networks in the detection and estimation stage

use different training sets in the learning process, they are trained more efficiently enabling a high-resolution identification of a source signal in azimuth angles from -90° to 90°, and elevation angles from -45° to 45°. In addition, the number of neurons in the input layer of each smaller network is reduced as only the first row of spatial covariance matrix is used to provide DOA estimates.

Compared to reference [6]-[8], where sectorisation model is applied for 1D DOA estimation, in this paper 2D case is considered. Using different training sets for two stages of the sectorisation model, lower number of training data is utilized and therefore, the training time of each smaller network is reduced. Besides, we here investigate a more complex problem, high–resolution 2D DOA estimation. The achieved accuracy of 2D DOA estimates is much better than the results reported in references [9]-[11].

The paper is organized as follows. In Section 2 data model for multiple antennas processing is given. In Sections 3 and 4 the structures of RBF and MLP neural networks and corresponding training procedures are described followed by the pre-processing of data for neural network training in Section 5. The use of single RBF network and sectorisation model for 2D DOA estimation is described in Section 6. Simulation results and comparison with 2D MUSIC algorithm are given in Section 7. The last section contains the concluding remarks.

2. Data Model for Antenna Processing

Let us consider a uniform rectangular array (URA) composed of $M \times N$ omnidirectional antenna elements (sensors), as shown in Fig. 1. Each antenna element is denoted by its coordinates (m, n), where $m = 0, 1, 2, \ldots M - 1$ and $n = 0, 1, 2, \ldots N - 1$. Elements of the URA are placed along the y- and z-directions with constant inter-element spacing of d_y and d_z, respectively. To avoid spatial aliasing, distance between adjacent elements in the URA is usually half a wavelength, $d_y = d_z = d = \lambda/2$.

A spherical coordinate system is used to represent direction of arrivals of incoming plane waves. For K narrowband signals, centered at frequency ω_0 that impinge on the URA from directions $\{(\varphi_1,\theta_1),(\varphi_2,\theta_2),\ldots,(\varphi_K,\theta_K)\}$ in azimuth and elevation, the signal received by the array elements can be written as

$$\mathbf{x}(t) = \mathbf{A}(\varphi,\theta)\mathbf{s}(t) + \mathbf{n}(t) \tag{1}$$

where x(t), n(t), and s(t) are given by

$$\begin{aligned}
\mathbf{x}(t) &= [x_{00}(t)\ x_{01}(t) \ldots x_{0N-1}(t)\ x_{10}(t)\ x_{11}(t) \ldots x_{M-1N-1}(t)]^T,\\
\mathbf{n}(t) &= [n_{00}(t)\ n_{01}(t) \ldots n_{0N-1}(t)\ n_{10}(t)\ n_{11}(t) \ldots n_{M-1N-1}(t)]^T,\\
\mathbf{s}(t) &= [s_1(t)\ \ s_2(t)\ \ldots\ \ s_K(t)]^T.
\end{aligned} \tag{2}$$

Vector of antenna array outputs is denoted by x(t), n(t) stands for the noise vector since signals incident on the array elements are assumed to have some noise associated with them, and s(t) represents the vector of source signals.

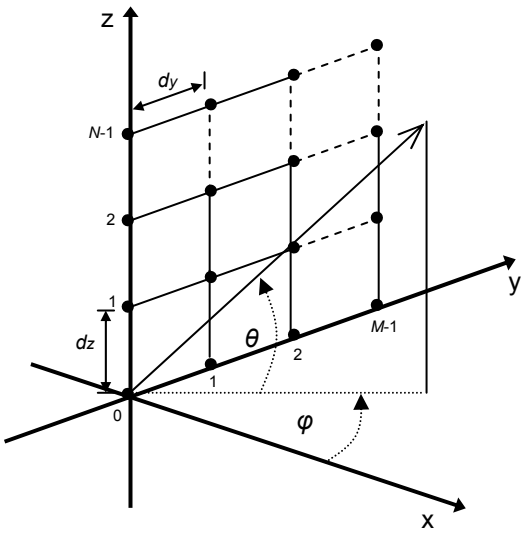

Fig. 1. Uniform rectangular array (URA).

The phase differences between signals collected by the array elements make it possible to calculate DOAs of incident signals.

If the phase reference point is located at $(m, n) = (0,0)$ then the phase of the k-th incident wave at the element with coordinates (m, n) can be determined as follows

$$\phi_{m,n}^{(k)}(\varphi_k,\theta_k) = \frac{2\pi}{\lambda}(d_y m\cos\theta_k \sin\varphi_k + d_z n\sin\theta_k). \tag{3}$$

Therefore, the steering vector of the k-th incident signal is given by

$$\begin{aligned}
\mathbf{a}^{(k)} &= [a_{00}^{(k)}\ a_{01}^{(k)} \ldots a_{0N-1}^{(k)}\ a_{10}^{(k)}\ a_{11}^{(k)} \ldots a_{mn}^{(k)} \ldots a_{M-1N-1}^{(k)}],\\
a_{mn}^{(k)} &= a_{mn}^{(k)}(\varphi_k,\theta_k) = e^{j\phi_{m,n}^{(k)}(\varphi_k,\theta_k)}
\end{aligned} \tag{4}$$

where $k = 1, 2, \ldots K$. $\mathbf{A}(\varphi,\theta)$ in (1) is a steering matrix whose columns are steering vectors towards K different directions of arrival and it can be written as follows

$$\mathbf{A}(\varphi,\theta) = [\mathbf{a}^{(1)}\ \ \mathbf{a}^{(2)}\ \mathbf{a}^{(3)} \ldots \mathbf{a}^{(k)} \ldots \mathbf{a}^{(K-1)}\ \ \mathbf{a}^{(K)}]. \tag{5}$$

In order to perform the DOA estimation, spatial covariance matrix $\mathbf{R}$ has to be determined [1]. The matrix $\mathbf{R}$ of the received noisy signals can be defined by

$$\begin{aligned}
\mathbf{R} &= E\{\mathbf{x}(t)\mathbf{x}(t)^H\} \ = \mathbf{A}E[\mathbf{s}(t)\mathbf{s}(t)^H]\mathbf{A}^H + E[\mathbf{n}(t)\mathbf{n}(t)^H]\\
&= \mathbf{A}\mathbf{R}_{xx}\mathbf{A}^H + \sigma_{noise}^2\mathbf{I} \ = \sum_{i=1}^{M*N}\lambda_i e_i e_i^H.
\end{aligned} \tag{6}$$

In (6), $\mathbf{R}_{xx} = E[(\mathbf{s}(t)\mathbf{s}^H(t))]$ stands for the correlation matrix of the received signals, λ_i are eigenvalues of the matrix $\mathbf{R}$, σ^2_{noise} is the variance of the statistically independent white noise signal, and H denotes the conjugate transpose. In practice, spatial covariance matrix $\mathbf{R}$ is unknown and it has to be estimated from a number of available data samples as

$$r_{ij} = \frac{1}{S}\sum_{k=1}^{S} x_i(k)\cdot x_j^*(k) \tag{7}$$

where $x_i(k)$ is the k-th sample of the i-th sensor, $x_j(k)$ is the k-th sample of the j-th sensor and S is the total number of samples.

According to (1) - (6), it can be observed that the URA performs the mapping $G: \mathbf{R}^K \rightarrow \mathbf{C}^{(M*N)}$ from the space of DOAs, $\Phi = [(\varphi_1, \theta_1), (\varphi_2, \theta_2), ..., (\varphi_K, \theta_K)]^T$ to the space of the array outputs $\{\mathbf{x}(t) = [x_{00}(t)\, x_{01}(t) \ldots x_{M-1N-1}(t)]^T\}$.

3. Radial Basis Function (RBF) Neural Networks

A neural network is a system composed of many simple processing elements operating in parallel. All processing elements (neurons) make their decisions simultaneously by taking into the consideration changes of the neural network global state. The function of the network is determined by its structure, connection weights and the processing performed at computing elements.

Neurons in a Radial Basis Function (RBF) neural network are organized into three layers, an input, an output as well as one hidden layer. Every neuron in each layer of the network is connected to every neuron in the adjacent forward layer, and no connections are permitted between the neurons belonging to the same layer. Each neuron is characterized by its transfer function and each connection between two neurons by a weight. Transfer functions of neurons of the input and output layers are usually linear whereas neurons of the hidden layer have radial basis transfer function that performs non-linear mapping.

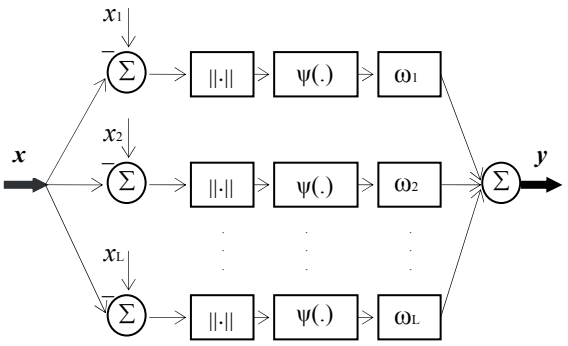

Fig. 2. Block diagram representation of the RBF neural network.

The main parameters of radial basis function are a centre vector and standard deviation (spread) [4], [5]. The mapping function depends on distance between the input vector and the centre vector. An RBF network with n-dimensional input $x \in R^n$ and m-dimensional output $y \in R^m$ can be represented by the weighted summation of a finite number of radial basis functions as follows

$$y = F(x) = \sum_{i=1}^{L} w_i \psi\left(\left\|x - x_i\right\|\right) \tag{8}$$

where $\psi\left(\left\|x - x_i\right\|\right)$ is the radial basis function of x, obtained by shifting $\psi\left(\left\|x\right\|\right)$ by x_i, L is a set of arbitrary functions and x_i are centers of the radial basis functions (Fig. 2).

The radial basis function $\psi\left(\left\|x - x_i\right\|\right)$ has its maximum at $x = x_i$ and monotonically decreases to zero as $\left\|x - x_i\right\|$ approaches to infinity. The term radial basis derives from the fact that this function is radially symmetric, which means that each node produces an identical output for all inputs lying at the fixed radial distance from centre. In other words, the radial basis function $\psi\left(\left\|x - x_i\right\|\right)$ has the same value for all neural inputs that lie on a hypersphere with the centre x_i. In (8), ψ is usually assumed to be unnormalized Gaussian function given by

$$\psi(x) = e^{\frac{-x^2}{2\sigma^2}} \tag{9}$$

where σ denotes the standard deviation of radial basis function. Gaussian function is highly nonlinear, and it is able to provide good characteristics for incremental learning.

The network is trained by a set of input-output pairs of data. At the beginning of the training process the network has no neurons in the hidden layer. Only one neuron is added in iteration with the center equal to the input vector that causes the maximum error. After that, weights between neurons are recalculated. This process continues until the previously defined criteria for the MSE (Mean Squared Error) is met or the maximum number of neurons in the hidden layer is reached. The spread (standard deviation) of the radial basis function is equal for all hidden neurons. As the best value of this parameter cannot be *a priori* known, it is usually experimentally determined through the training of a number of neural networks and comparing their performance. The size of the RBF network (number of neurons in the hidden layer) is known at fully trained network. Once trained, the network is able to give accurate responses to those inputs that have not been presented to the network in the training process. The test set is taken from the same distribution as the inputs used in the training set. Accuracy of the trained RBF neural network can be expressed using statistical parameters such as worst case error (WCE (%)), average case error (ACE (%)) and Pearson Product-Moment correlation coefficient. Correlation coefficient r between reference values and network responses can be defined by

$$r = \frac{\sum \left(p_i - \overline{p_i}\right)\left(q_i - \overline{q_i}\right)}{\sqrt{\sum \left(p_i - \overline{p_i}\right)^2 \sum \left(q_i - \overline{q_i}\right)^2}} \tag{10}$$

where p_i represents the reference value, q_i is the ANN computed value, p is the reference sample mean, and q is the ANN sample mean. The correlation coefficient is an indicator of how well the modeled values match the actual ones. If the correlation coefficient is close to one then the neural network has an excellent predictive ability whereas r close to zero indicates poor performance of the network. Finally, the network demonstrating the best test statistics is chosen for simulations and further analysis.

4. Multilayer Perceptron (MLP) Neural Networks

MLP neural networks are usually consisted of an input layer, an output layer as well as several hidden layers (Fig. 3). With one or two hidden layers, they can approximate virtually any input-output mapping. Due to this ability MLP neural networks are suitable for modeling of high-dimensional and highly non-linear problems [12], [13].

In this work, MLP neural networks (MLP-NNs) with two hidden layers are utilized in the detection stage of the proposed sectorisation model. MLP-NNs make powerful classifiers that may provide superior performance compared with other classifiers. However, difficulties with MLP-NNs include long training times and local minima. In the particular case, training convergence speed of this network type is slower but more accurate than is the case with RBF-NNs. That is the main reason of application of MLP-NNs in the detection stage. To design a learning system it is customary to divide example samples into two sets, a training set to design a classifier and a test set, which is subsequently used to predict the performance when previously unseen examples are applied. The most known training procedure is the backpropagation algorithm and its modifications such as quasy-Newton or Levenberg-Marquardt algorithms [4]. Following this procedure, the output of the l-th layer of the network can be written as

$$Y_l = F(W_L Y_{l-1} + B_l) \tag{11}$$

where Y_l and Y_{l-1} are outputs of the l-th and (l-1)-th layer, respectively, W_l is a weight matrix between the (l-1)-th and l-th layer and B_l is a bias matrix between the (l-1)-th and l-th layer. Function F is the activation function of each neuron and it is linear for input and output layer and sigmoid (tan-sigmoid in the particular case) for hidden layers

$$F(u) = (1-e^{-u})/(1+e^{-u}). \tag{12}$$

After the output vectors are determined, they are compared to the target values and errors are computed. Error derivatives are then calculated and summed up for each weight and bias until whole training set has been presented to the network.

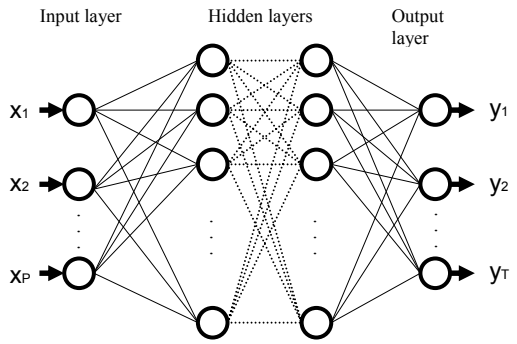

Fig. 3. Multilayer Perceptron (MLP) neural network.

The error derivatives are used to update the weights and biases for neurons in the model. The training process continues until errors are lower than the prescribed values or until the maximum number of epochs is reached [4]. Once trained, the network provides a fast response for different input vectors, even for those not included in the training set. Accuracy of the trained MLP neural network can be also expressed in terms of WCE, ACE or correlation coefficient between reference values and network responses [4], [5].

5. Pre-processing of Data

The architecture of a system using one RBF neural network for 2D DOA estimation is shown in Fig. 4. Application of artificial neural networks in the area of DOA estimation is based on the inverse mapping to the one that antenna array performs. That is the mapping $G: \mathbf{C}^{(M*N)} \rightarrow \mathbf{R}^K$ from the space of antenna array outputs $\{\mathbf{x}(t) = [x_{00}(t)\, x_{01}(t) \ldots x_{M-1N-1}(t)]^T\}$ to the space of DOAs $\Phi = [(\varphi_1, \theta_1), (\varphi_2, \theta_2), \ldots, (\varphi_K, \theta_K)]^T$. Input data of RBF neural network is a spatial covariance matrix **R** of the antenna array outputs, and DOAs of incident signals are ANN responses. Number of neurons in the input layer of the network depends on the dimensionality of **R** matrix. As **R** is a (M*N) × (M*N) square matrix and keeping in mind that ANNs cannot operate with complex numbers, there should be $2(M*N)^2$ neurons in the input layer of the network. Since covariance matrix depends both on azimuth and elevation angles, separate training sets cannot be used as network input to train only azimuth, or only elevation. Consequently, dimensionality of input layer significantly increases when large antenna arrays are employed at the receiver.

In this paper, a dimension-degraded training set is used to develop both MLP and RBF neural network models. For that purpose, only the first row of covariance matrix is used to represent signals at the array output [7]. All inputs are organized into a 2(M*N) - 1 element vector **b** that is, before it is applied to the input layer of the neural network, normalized with its norm, **z** = **b**/||**b**||. Therefore, the dimensionality of input vectors is significantly reduced allowing efficient training of neural network models.

6. DOA Estimation using Neural Networks

6.1 Single RBF Neural Network

Instead of 2D MUSIC algorithm single RBF neural network can be used to estimate DOAs of source signals. Unlike 2D MUSIC, the neural network does not perform eigen-decomposition of spatial covariance matrix. It requires only a minor pre-processing before the elements of covariance matrix are applied as input to the network. After the post-processing of the neural network response

(that usually assumes only denormalization process) DOAs of source signals are provided (Fig. 4).

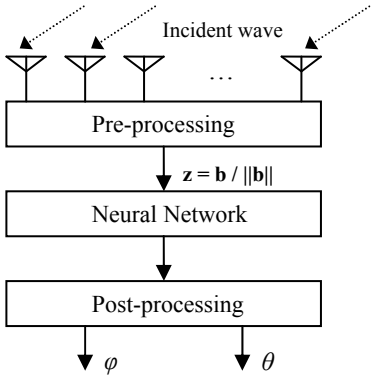

Fig. 4. DOA estimation employing a neural network.

6.2 Sectorisation Model

To provide high-resolution 2D DOA estimates, a sectorisation model is proposed. A concept of the sectorisation model for high-resolution 2D DOA estimation is shown in Fig. 5, where S_E and S_A represent the number of plane sectors in elevation and azimuth, respectively.

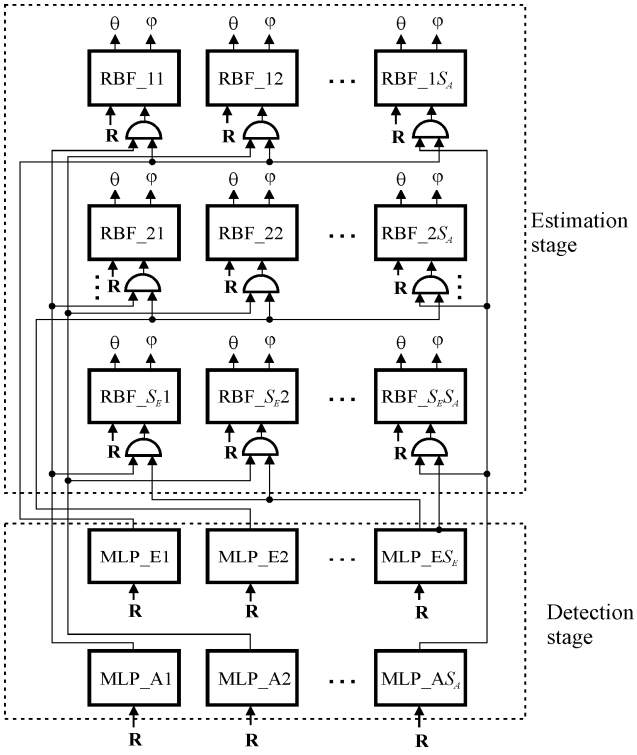

Fig. 5. Detection and estimation stages of the sectorisation model.

The main idea is to quickly detect the presence of a source in a sector and after that, to provide high-resolution 2D DOA estimate in such identified narrow space (space sector). Therefore, two stages in the sectorisation model are performed: detection stage for detection of the source in elevation and azimuth, respectively, and one estimation stage for 2D DOA estimation. The MLP neural networks in the detection stage act as classifiers. Output of a MLP network is 0 when the tracked source is outside the observed sector associated with this network, and 1 for the source inside the sector. One MLP network for elevation and one MLP network for azimuth, both with output 1, are used in the estimation stage to activate RBF network corresponding to the detected space sector. As a result, DOA of high resolution is obtained.

7. Modeling Results

To illustrate performance of the proposed approaches computer simulations of the signal processing performed by neural models and 2D MUSIC algorithm have been done. Simulations were run in MATLAB software. The following parameters in simulations are assumed: uniform rectangular array (URA) composed of 16 identical omnidirectional elements, half a wavelength inter-element spacing, $d = \lambda/2$, 1024 snapshots of BPSK (Binary Phase Shift Keying) modulated signal, and Signal to Noise (SNR) ratio of 20 dB.

7.1 Single RBF Neural Network Model

In this section, a RBF neural network is trained to track a source in azimuth and elevation. To collect input-output training vectors, it is supposed that the source is moving in steps of 2° in azimuth [-90°-90°] and elevation [-45°-45°]. In a similar way, the test set is formed for the angular positions separated by 3.3°. A number of RBF neural networks are trained and the network demonstrating the best performance (with 219 neurons in the hidden layer), is chosen for simulations (Tab. 1). A number of DOAs and the quality of the associated estimates are shown in Fig. 6. The black circles represent the reference DOAs, whereas the white circles represent the appropriate RBF neural network responses. It can be concluded that the results provided by RBF ANN modeling are in good agreement with the reference angular positions. The simulation run for DOA estimation using single RBF neural network is done in a matter of seconds (Intel(R) Core(TM) 2 Quad CPU computer with 8 GB RAM).

RBF neural model	WCE [%]	ACE [%]	r
RBF1_1 (spread 1.90)	4.0401	0.3340	0.9999
RBF1_2 (spread 1.80)	4.2029	0.3322	0.9998
RBF1_3 (spread 1.65)	4.1812	0.3342	0.9998
RBF1_4 (spread 1.75)	4.4449	0.3378	0.9998
RBF1_5 (spread 1.35)	4.5677	0.3609	0.9998

Tab. 1. Single RBF neural network test statistics.

If the higher accuracy of 2D DOA estimates is required then a very large training set must be used to train the single neural network. The whole process can appear as very time-consuming, with an uncertain outcome.

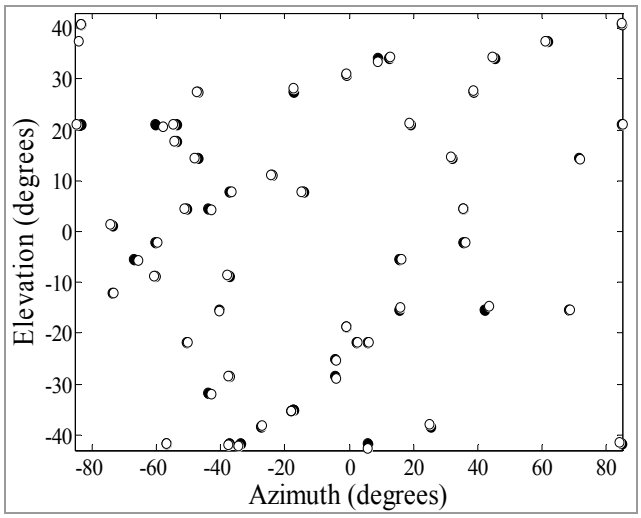

Fig. 6. RBF network results for test samples compared to referent DOAs (○ – RBF network response, ● – referent DOA).

7.2 Sectorisation Model

In order to generate the sectorisation model, the observed space is divided into three sectors in elevation (S_E=3), each 30º wide ([-45º,-15º], [-15º, 15º], [15º, 45º], and then five sectors in azimuth (S_A=5) ([-90º,-60º], [-60º,-20º], [-20º, 20º], [40º, 60º], [60º, 90º]). The procedure to train MLP and RBF networks used in the detection and estimation stages is described as follows. First, data taken with a fine step close to the borders of the sector and a coarser step towards its centre are used to train the MLP networks in the detection stage. After that, for the user belonging to the sector, more refined data are used to train the RBF network in the estimation stage giving as a result a high-resolution DOA estimate. Following the described procedure, several smaller data sets are formed allowing an efficient training of both MLP and RBF networks instead of one large data set when single RBF network is employed.

A number of MLP networks in the detection stage, aimed to disclose the source in the elevation and azimuth sectors, are developed. As the size of hidden layers in a network cannot be a priori known, the optimum number of neurons is usually found through an investigation. Namely, an iterative process is applied in order to dynamically adjust the network configuration. This procedure starts with a minimum network, then adds hidden neurons and recalculates weights and biases during training. As the iterative process converges to the solution, the network with good test statistics is obtained.

If the number of hidden neurons is further increased (after an optimum configuration is found), the network will give excellent results for training samples but its generalization capabilities - results for test samples, will be deteriorated.

Finally, models that best approximate the presence of the source are chosen for simulations. In Tab. 2, test characteristics of the models for the elevation sector [-15º, 15º] are presented as an illustration. MLP network having 22 neurons in both hidden layers is applied for test samples that have not been used in the training process. The corresponding response of the network is shown in Fig. 7. In Tab. 3, performances of the best MLP networks trained for the detection in azimuth sector [-20°, 20°] are shown. MLP_2-22-22 network is simulated for test points and its response is depicted in Fig. 8. The training time of the network in the elevation sector is 17 s, and 10 s for the network in the azimuth sector peak (Intel(R) Core(TM)2 Quad CPU computer with 8 GB RAM).

MLP neural model	WCE [%]	ACE [%]	r
MLP_E-22-22	2.3362	0.1370	1.0000
MLP_E-12-11	2.3628	0.0634	1.0000
MLP_E-14-11	2.8050	0.0658	1.0000
MLP_E-16-16	2.9050	0.3598	1.0000
MLP_E-30-16	3.1683	0.1777	1.0000

Tab. 2. MLP neural network test statistics for the elevation (E) sector [-15º, 15º].

MLP neural model	WCE [%]	ACE [%]	r
MLP_A-22-22	1.7102	0.1359	1.0000
MLP_A-20-20	2.5157	0.0365	1.0000
MLP_A-14-11	3.1012	0.0657	1.0000
MLP_A-16-12	3.5327	0.0490	1.0000
MLP_A-18-18	3.8951	0.2885	0.9999

Tab. 3. MLP neural network test statistics for the azimuth (A) sector [-20°, 20°].

RBF neural model	WCE [%]	ACE [%]	r
RBF_1 (spread 1.95)	2.7997	0.3341	0.9999
RBF_2 (spread 1.15)	2.9638	0.3498	0.9999
RBF_3 (spread 2.00)	3.0541	0.3600	0.9998
RBF_4 (spread 1.45)	4.8670	0.3617	0.9998
RBF_5 (spread 1.70)	2.6690	0.3752	0.9998

Tab. 4. RBF neural network test statistics – sectorisation model.

The training data for the RBF network are taken in steps of 0.5° in azimuth and elevation in order to increase the accuracy of DOA estimates. Therefore, the training set for one RBF network in the sectorisation model contains 4941 samples. As an illustration, if single RBF network is employed for DOA estimation then the obtained training set has much larger size (65 341 samples).

RBF network demonstrating the best test statistics (WCE = 2.7997 %, ACE = 0.3341 %, r = 0.9999), is used in the simulation process (Tab. 4). The hidden layer of the chosen network is composed of 81 neurons. The training time of an RBF network in the estimation stage is about

60 s. As shown in Fig. 9, angular positions of the source estimated by the RBF neural network are in good agreement with the actual ones that proves the performance of the proposed method.

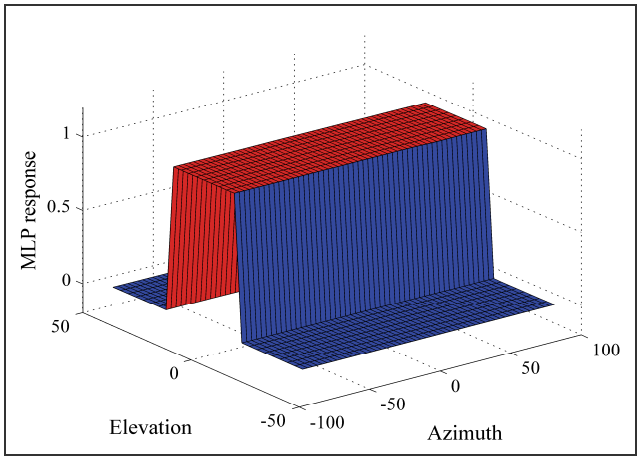

Fig. 7. MLP neural network response in the elevation sector detection stage for test samples.

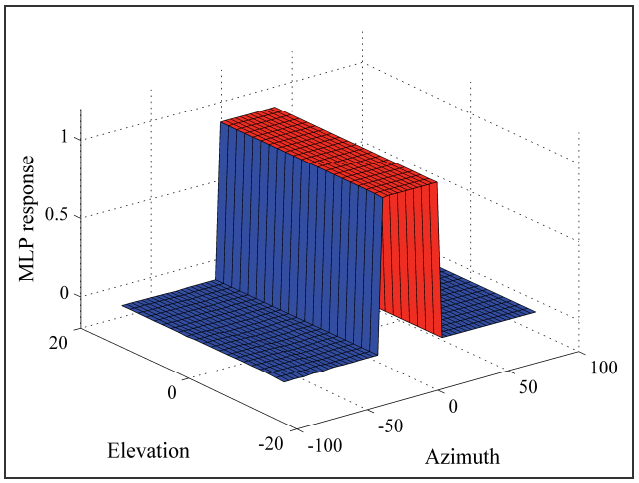

Fig. 8. MLP neural network response in the azimuth sector detection stage for test samples.

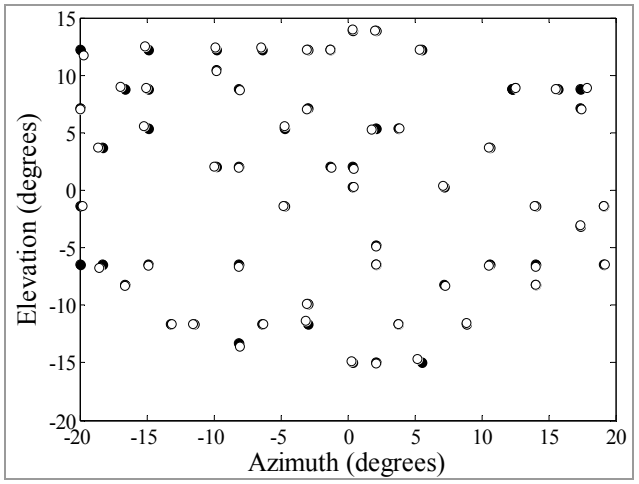

Fig. 9. Results of the sectorisation model results for test points (○ – sectorisation model response, ● – referent DOA).

In addition, in Fig. 10 and 11 there are results of the sectorisation model and 0.5º-resolution 2D MUSIC algorithm plotted for randomly selected azimuth and elevation angles. It can be concluded that the proposed sectorisation model has performance comparable to that of 2D MUSIC. However, the proposed model provides DOA estimates in a matter of seconds while 2D MUSIC needs much more time (approximately 20 s) to search the for the spectrum peak (Intel(R) Core(TM)2 Quad CPU computer with 8 GB RAM).

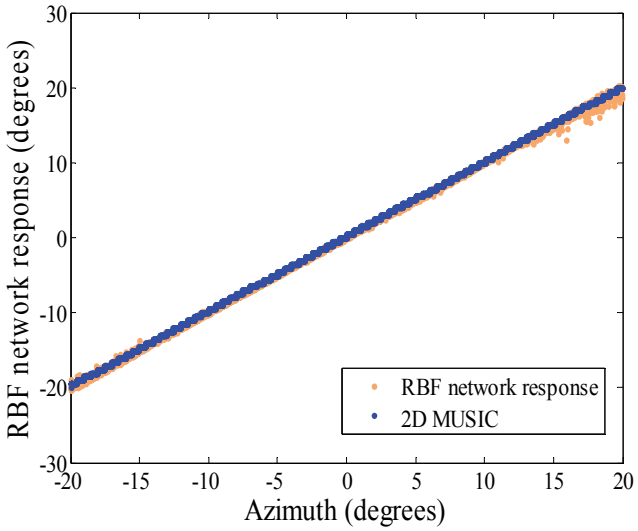

Fig. 10. Correlation diagram of the sectorisation model and 2D MUSIC DOAs for azimuth angles.

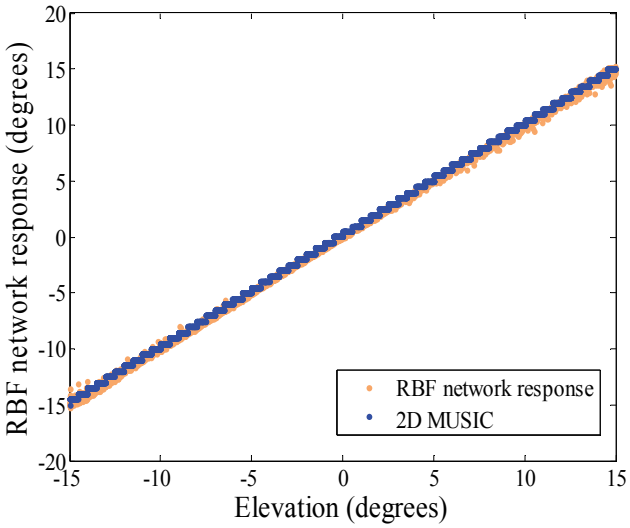

Fig. 11. Correlation diagram of the sectorisation model and 2D MUSIC DOAs for elevation angles.

8. Conclusion

In this paper, efficient neural network-based models for high-resolution 2D DOA estimation are proposed. A key advantage of the presented models over the super-resolution 2D MUSIC algorithm is their ability to provide accurate 2D DOA estimates almost instantaneously as they

avoid complex matrix calculations. Therefore, both models (single RBF and sectorisation model) are more suitable for real-time implementation in comparison to 2D MUSIC. It is demonstrated that sectorisation model provides smaller DOA estimation error and therefore, better resolution than the single RBF model. At the same time, sectorisation model significantly reduces the training time of neural models.

Acknowledgements

This work was supported by the project TR-32052 of the Serbian Ministry of Education and Science, and the project CARE (Coordinating the Antenna Research in Europe) of the Institut für Hochfrequenztechnik und Elektronik of Karlsruhe Institute of Technology (KIT), Germany.

References

[1] SCHMIDT, R. Multiple emitter location and signal parameter estimation. *IEEE Transactions on Antennas and Propagation*, 1986, vol. 34, no. 3, p. 276-280.

[2] ROY, R., KAILATH, T. ESPRIT-estimation of signal parameters via rotational invariance techniques. *IEEE Transactions on Acoustics, Speech and Signal Processing*, 1989, vol. 37, no. 7, p. 984 – 995.

[3] OTTERSTEN, B., VIBERG, M., KAILATH, T. Performance analysis of the total least squares ESPRIT algorithm. *IEEE Transactions on Signal Processing*, 1991, vol. 39, no. 5, p. 1122-1134.

[4] ZHANG, Q. J., GUPTA, K. C. *Neural Networks for RF and Microwave Design*. Artech House, 2000.

[5] CHRISTODOULOU, C. G., GEORGIOPOULOS, M. *Application of Neural Networks in Electromagnetics*. Artech House, 2000.

[6] EL ZOOGHBY, A. H., CHRISTODOULOU, C. G., GEORGIOPOULOS, M. A neural network-based smart antenna for multiple source tracking. *IEEE Transactions on Antennas and Propagation*, 2000, vol. 48, no. 5, p. 768 – 776.

[7] ÇAYLAR, S., LEBLEBICIOĞLU, K., DURAL, G. A new neural network approach to the target tracking problem with smart structure. In *Proceedings of IEEE AP-S International Symposium and USNC/URCI meeting*, Albuquerque (USA), 2006, p. 1121-1124.

[8] WANG, M., YANG, S., WU, S., LUO, F. A RBFNN approach for DOA estimation of ultra wideband antenna array. *Neurocomputing-Elsevier*, 2008, vol. 71, no. 4-6, p. 631-640.

[9] JORGE, N., FONSECA, G., COUDYSER, M., LAURIN, J.-J., BRAULT, J.-J. On the design of a compact neural network-based DOA estimation system. *IEEE Transactions on Antennas and Propagation*, 2010, vol. 58, no. 2, p. 357-366.

[10] MATSUMOTO, T., KUWAHARA, Y. 2D DOA estimation using beam steering antenna by the switched parasitic elements and RBF neural network. *Electronics and Communications in Japan (Part I: Communications)*, 2006, vol. 89, no. 9, p. 22-31.

[11] HONGGUANG, C., BIAO, L., ZHENKANG, S. Efficient network training method for two-dimension DOA estimation. In *Proceedings of the 4th International Conference on Computer and Information Technology (CIT '04)*. Wuhan (China), 2004, p. 1028 – 1032.

[12] STANKOVIĆ, Z., MILOVANOVIĆ, B., DONČOV, N. Hybrid empirical-neural model of loaded microwave cylindrical cavity. *Progress in Electromagnetics Research, PIER*, 2008, vol. 83, p. 257-277.

[13] SAREVSKA, M., MILOVANOVIĆ, B., STANKOVIĆ, Z. Reliability of radial basis function - neural network smart antenna. In *Proceedings of the 9th WSEAS International Conference on Communications*. Athens (Greece), 2005.

About Authors …

Marija AGATONOVIĆ received the Dipl.-Ing degree in Electrical Engineering from the Faculty of Electronic Engineering, University of Niš, Serbia, in 2006. She is a PhD student at the University of Niš and a scholarship holder of the Serbian Ministry of Education and Science. In 2011, she received the CARE (Coordinating the Antenna Research in Europe) grant and conducted both theoretical and experimental research at the Institut für Hochfrequenztechnik und Elektronik (IHE), Karlsruhe Insititute of Technology, Germany. Her research areas are artificial neural networks and their applications in electromagnetics and signal processing.

Zoran STANKOVIĆ received the Dipl.-Ing., M.Sc., and Ph.D. degrees from the Faculty of Electronic Engineering, University of Nis, Serbia, in 1994, 2002 and 2007, respectively. Currently, he is a Research and Teaching Assistant at the Department of Telecommunications, Faculty of Electronic Engineering, Serbia. His research interests include neural networks applications in the field of electromagnetics, wireless communications systems and computer communications. Dr. Stanković was the recipient of the National MTT Society award in 2005 for the outstanding scientific results in the area of microwave techniques. He is a member of the International Society for Advanced Research since 2005.

Nebojša DONČOV received the Dipl.-Ing., M.Sc., and Ph.D. degrees from the Faculty of Electronic Engineering, University of Nis, Serbia, in 1995, 1999 and 2002, respectively. Currently, he is an Associate Professor at the Faculty of Electronic Engineering, Serbia. His research interests are in computational and applied electromagnetics with a particular emphasis on TLM and neural networks applications in microwaves and EMC. Dr. Dončov was the recipient of the International Union of Radio Science (URSI) Young Scientist Award in 2002.

Leen SIT received the B.Eng(Hons)Electronic from the University Sains Malaysia in 2006. She received the dual Masters in Information and Communication Technologies in Université Catholique de Louvain (UCL), Belgium, and Üniversität Karlsruhe (TH), Germany in 2007. Since the completion of her Masters in 2009 she has been a Research Assistant at the Institut für Hochfrequenztechnik und Elektronik (IHE) at Karlsruhe Institute of Technology. Her current research area includes automotive radar systems, wireless communication, antennas and propagation.

Bratislav MILOVANOVIĆ received the Dipl.-Ing., M.Sc., and Ph.D. degrees from the Faculty of Electronic Engineering, University of Nis, Serbia, in 1972, 1975 and 1979, respectively. From 1972 onwards he was promoted at the Faculty of Electronic Engineering to all academic positions to full Professor (1990). Since 1994 he is the Head of the Department of Telecommunications. Also, he was the Vice-dean in the period from 1987 - 1991 and the Dean of the Faculty of Electronic Engineering from 1994 - 1998. His present research work is in the field of telecommunications, particularly in the field of microwave theory and techniques, computational electromagnetics and neural networks applications. He is a general chairman of of the IEEE conference TELSIKS, a member of Serbian Scientific Society, a full member of the Academy of Engineering Sciences of Serbia, a president of National MTT Society and the president of IEEE MTT Chapter of Serbia and Montenegro.

Thomas ZWICK received the Dipl.-Ing. (M.S.E.E.) and Dr.-Ing. (Ph.D.E.E.) degrees from the Universität Karlsruhe, Karlsruhe, Germany, in 1994 and 1999, respectively. From 1994 and 2001, he was a Research Assistant at the Institut für Höchstfrequenztechnik und Elektronik (IHE), Universität Karlsruhe. From 2001 to 2004, he was at the IBM T. J. Watson Research Center, Yorktown Heights, NY. From 2004 to 2007, he was with Siemens AG, Lindau, Germany. Since 2007, he has been the Director of the IHE, Karlsruhe Institute of Technology, Karlsruhe. He is the author or coauthor of more than 100 technical papers and more than ten patents. His research interests include wave propagation, millimeter wave antenna design and wireless communications.